

Dichlorodimethylsilane as an Anti-Stiction Monolayer for MEMS: A Comparison to the Octadecyltrichlorosilane Self-Assembled Monolayer

W. Robert Ashurst, Christina Yau, Carlo Carraro, Roya Maboudian, and Michael T. Dugger

Abstract—This paper presents a quantitative comparison of the dichlorodimethylsilane (DDMS) monolayer to the octadecyltrichlorosilane (OTS) self-assembled monolayer (SAM) with respect to the film properties and their effectiveness as anti-stiction coatings for micromechanical structures. Both coatings have been evaluated in several ways, including atomic force microscopy (AFM), contact angle analysis (CAA), work of adhesion by cantilever beam array (CBA) technique and coefficient of static friction using a sidewall testing device. While water and hexadecane contact angles are comparable, the DDMS coated microstructures exhibit higher adhesion than OTS coated ones. Furthermore, coefficient of static friction data indicate that the DDMS films are not as effective at lubrication as the OTS SAM's are, although both exhibit much improvement over chemical oxide. However, AFM data show that the samples which receive DDMS treatment accumulate fewer particles during processing than those which receive the OTS SAM treatment. The thermal stability of the DDMS film in air far exceeds the OTS SAM, as the DDMS remains very hydrophobic to temperatures upwards of 400 °C. [559]

Index Terms—MEMS, self-assembled monolayer, stiction, tribology.

I. INTRODUCTION

THE large surface-area-to-volume ratios of surface and bulk micromachined micromechanisms bring the role of stiction into the foreground, as adhesion of these mechanisms to adjacent surfaces is a major failure mode for MEMS [1]–[5], [21]. Stiction is a term that has been applied to the unintentional adhesion of compliant microstructure surfaces when restoring forces are unable to overcome interfacial forces such as capillary, van der Waals and electrostatic attractions. Release stiction, the adhesion of surface-micromachined structures to the underlying substrate following the final sacrificial layer etch, is caused primarily by liquid capillary forces. Engineering solutions to this problem include a variety of techniques which have been reviewed elsewhere [1]–[5], [21]. Most of these techniques, however, do not prevent adhesion from occurring during microma-

chine operation. Microstructure surfaces may come into contact unintentionally through acceleration or electrostatic forces, or intentionally in applications where surfaces impact or shear against one another. When adhesive attractions exceed restoring forces, surfaces permanently adhere to each other causing device failure—a phenomenon known as in-use stiction. In addition, it is known that on the microscale, friction is strongly dependent upon adhesion [6].

In order to alleviate these adhesion-related problems, both the topography and the chemical composition of the contacting surfaces must be controlled. Alley *et al.* considered the use of self-assembled monolayers for alleviating adhesion in polycrystalline silicon (polysilicon) microstructures [7]. In particular, they examined self-assembled monolayer coating derived from the precursor molecule octadecyltrichlorosilane ($\text{CH}_3(\text{CH}_2)_{17}\text{SiCl}_3$, OTS) using arrays of microfabricated cantilever beams. They showed promising results for alleviating release-related stiction and suggested these SAM's as a potential post-release anti-stiction lubricant. However, due to the stiffness of the structures investigated, no quantitative measure of the stiction properties of SAM-coated surfaces could be made at that time. Houston *et al.* integrated the OTS coating with the microstructure release process and showed that release stiction is effectively eliminated and in-use stiction is reduced by three orders of magnitude with respect to conventional oxidation release procedures [8].

In addition to the OTS precursor molecule, there are many other molecules of the form RSiCl_3 and $\text{R,R}'\text{SiCl}_2$ which are used to produce oriented hydrophobic monolayers on silicon surfaces, where R and R' denote aliphatic carbon chains. In fact, it has been demonstrated that the most effective reagents to produce hydrophobic coatings on oxidized silicon surfaces are perfluorinated alkyltrichlorosilanes [9]. For example, a SAM coating formed from 1H, 1H, 2H, 2H-perfluorodecyltrichlorosilane ($\text{CF}_3(\text{CF}_2)_7(\text{CH}_2)_2\text{SiCl}_3$, FDTS) has a critical surface tension as low as 6 mJ/m² in comparison to 15 and 22 mJ/m² for Teflon and OTS coatings, respectively [10]. Indeed, lower values for the apparent work of adhesion are reported for FDTS in comparison to OTS [9].

However, when evaluating the anti-stiction properties of a molecular film, consideration must be given to all aspects of the film formation process, including possible harm to structures resulting from particulates or chemical by-products, packaging environment and conditions, film longevity and reliability. For example, some packaging processes require that the film be thermally stable upwards of 350 °C in various ambients, in-

Manuscript received April 7, 2000; revised August 14, 2000. This work was supported in part by the National Science Foundation under Grant DMI-9908169), Sandia National Labs, and in the form of a graduate fellowship (WRA), and in part by the Arnold and Mabel Beckman Foundation. Subject Editor, D. J. Harrison.

W. R. Ashurst, C. Yau, C. Carraro, and R. Maboudian are with the Department of Chemical Engineering, University of California at Berkeley, Berkeley, CA 94720-1492 USA.

M. T. Dugger is with the Sandia National Laboratories, Albuquerque, NM 87185 USA.

Publisher Item Identifier S 1057-7157(01)01597-9.

cluding oxidizing environments. The OTS SAM has been shown to be stable in oxidizing ambients for temperatures up to 225 °C, and microstructures that have undergone the OTS SAM treatment typically exhibit particles that arise from bulk polymerization of the precursor molecules [11]. The FDTS coating is found to be stable up to 400 °C in an oxidizing environment, [9] but it is even more susceptible to particulate contamination than the OTS SAM. Oh *et al.* have recently examined the use of dichlorodimethylsilane ($\text{Cl}_2\text{Si}(\text{CH}_3)_2$, DDMS) as an anti-stiction coating [12]. They have determined that the DDMS monolayer retains its hydrophobicity in an oxidizing ambient up to 450 °C for a short time period, and at room temperature for over six months [12]. They proposed that the DDMS film might exhibit superior anti-stiction behavior when compared to the OTS SAM. Additionally, due to the reduced number of reactive sites per precursor molecule, (two for DDMS versus three for OTS) bulk polymerization may be substantially reduced, given equivalent processing conditions.

In this paper, we present a quantitative comparison of the DDMS monolayer to the widely accepted anti-stiction benchmark, namely the OTS SAM. Items studied in detail for this work include contact angle analysis (CAA), apparent work of adhesion found from the cantilever beam array technique (CBA), coefficient of static friction using a sidewall testing device, film thermal stability in an oxidizing ambient, and particulate accumulation during monolayer processing. Our results indicate that although DDMS is thermally more stable than OTS and is less susceptible to particulate accumulation, the OTS coating exhibits superior anti-adhesion and lower friction characteristics.

II. EXPERIMENTAL

A. Anti-Stiction Coating Procedures

The films studied in this work are the OTS SAM and the DDMS monolayer. Both precursor molecules employ chlorosilane binding chemistry, but the OTS has three Si-Cl bonds whereas the DDMS has only two. Additionally, the OTS has one long (18-carbon) alkane chain bound to the chlorosilane group whereas the DDMS has two short (one-carbon) methyl groups. The procedure used to form both the OTS and the DDMS monolayers has been outlined in [9] and [12], but has been slightly modified, and is presented here for completeness. For reference, structures are also prepared without any anti-stiction coating, i.e., oxidized surfaces.

The OTS and the DDMS monolayer coating procedures are carried out identically, with the only exception being the precursor molecule used. The iso-octane, used as the solvent for the precursor molecules, is anhydrous (Aldrich Chemical Company 99.8%+) to help prevent bulk polymerization. The OTS is from Aldrich Chemical Company, 95%, and the DDMS is from Gelest, 99+%. Deionized (DI) water is obtained from a Barnstead NanoPure II System, with 18 M Ω -cm resistivity. All the other chemicals are standard solvent grade, Certified A.C.S.

Processing of the microstructure die begins with the sacrificial layer etch, carried out with HF. The HF and etch products are then rinsed away with DI water. This and all other displacement rinses are carried out using a “fill/drain” approach via a

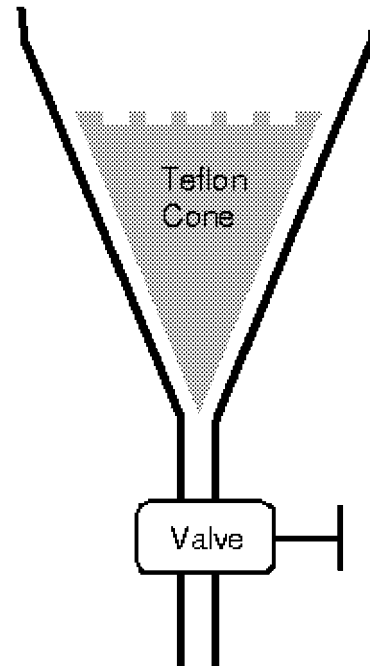


Fig. 1. Schematic diagram of the “fill/drain” apparatus.

funnel device (Fig. 1), which is further described in the Results and Discussion section. HF treatment leaves the polysilicon surfaces hydrogen-terminated, but they must be oxidized for the chlorosilane binding chemistry to occur. For this, hot (~90 °C) 30% hydrogen peroxide is poured into the funnel and allowed to sit for 15 min. The peroxide is then partially displaced with DI water, followed by complete displacement with isopropyl alcohol (IPA), such that the water and peroxide are completely removed. The IPA is similarly displaced with iso-octane, and the die are transferred into a conditioned coating solution in a glass coating dish which had been previously treated with the appropriate precursor molecule. The die remained in the coating solution, covered for one hour, and is then transferred to pure iso-octane. The iso-octane is subsequently displaced with IPA, and the IPA similarly displaced with DI water. All micromachine chips are removed from the liquid state only at the last step. Removal of the die from DI water is carried out such that the die surface is perpendicular to the liquid surface, and is performed in one slow but continuous motion.

The procedure carried out for the oxidized microstructures consists of the standard release, followed by surface oxidation with 30% H_2O_2 at 90 °C for 10 min. The structures are then rinsed in DI water and either supercritically dried or removed directly from water and air-dried. Air-dried structures, prone to release stiction, are then manually probed to release them from the substrate before testing.

B. Cantilever Beam Array

CBA technique is employed to characterize the release and in-use stiction properties of the anti-stiction coatings [13], [14]. The array (Fig. 2) consists of 20- μm -wide cantilever beams, which extend from 150 to 1700 microns in length, and are 2 μm above the surface. The beam lengths are incremented by 50 μm . The structural polysilicon layer is 2.5- μm thick. These

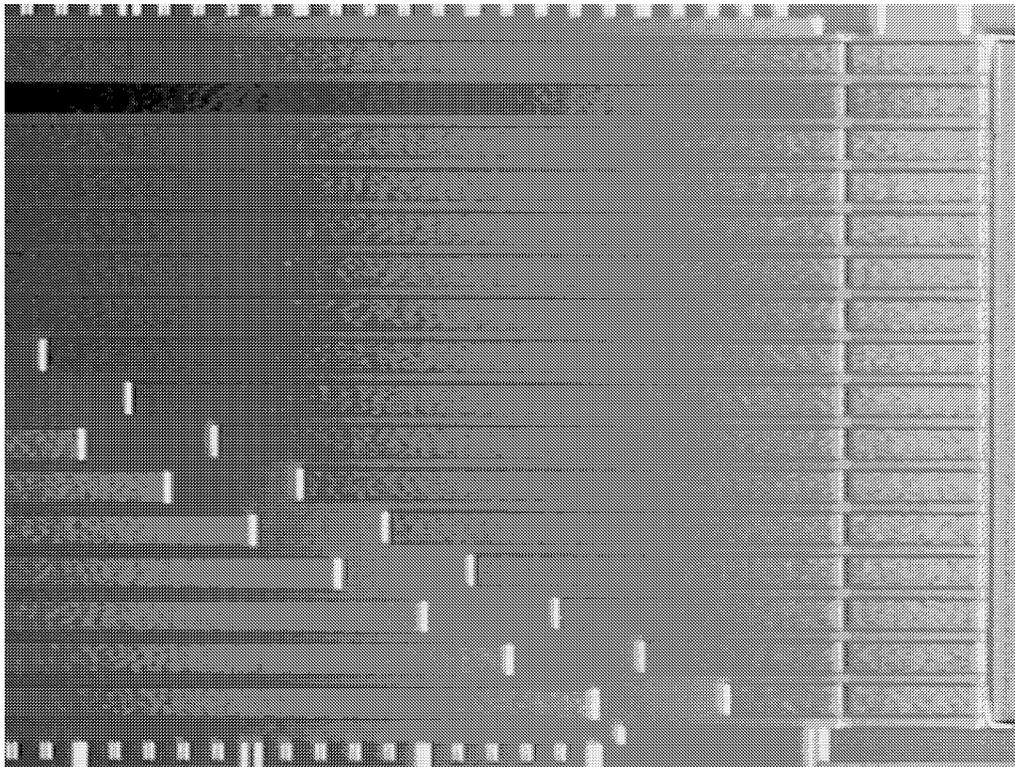


Fig. 2. CBA as seen under differential interference contrast microscopy. The darkened beam ($850\ \mu\text{m}$ long) is the only one that is adhered to the substrate.

structures are fabricated at Sandia National Laboratories, Albuquerque, NM, using standard surface micromachining techniques. Complete details of the fabrication process can be found elsewhere [15].

In order to quantify in-use stiction, the beams are electrostatically brought into contact with the underlying substrate by applying a periodic voltage of 100 V to an $80\text{-}\mu\text{m}$ actuation pad located near the anchor region. The beams are actuated with a very low frequency (0.3 Hz) square wave signal at 20% duty for five cycles. After the fifth complete cycle the drive signal is turned off, and the measurements are taken. Differential interference contrast microscopy is used to determine if beams are adhered to the substrate before and after actuation.

C. Coefficient of Static Friction on Micromachine Sidewalls

Sidewall static friction data are obtained via a test structure that consists of a beam that can be brought into contact and rubbed against a rounded, fixed post. Details on the fabrication of this test structure can be found elsewhere [16]. Photos of the test structure are given as Fig. 3(a) and (b), where relevant components of the device are labeled by arrows. Previously, this structure has been used for *kinetic* friction coefficient measurement [16]. In this paper, we report on the use of this test structure to determine the coefficient of *static* friction.

The actuation of the test device is performed as follows. First, a dc normal potential (V_N) of 80–100 V is applied to the so-called normal comb drive so that a normal force is generated on the anchored post. Then a small (~ 1 V) dc potential is applied to the so-called tangential comb drive so as to cause a right to left (with respect to Fig. 3) tangential force. This tangential potential (V_T) is then slowly ramped up (~ 1 V/s) until

slippage of the sidewall beam occurs. With knowledge of the normal and tangential forces, the coefficient of static friction μ_s , defined as the ratio of tangential force to normal force at the onset of slippage, can be determined. Since this device has not been described for use in this manner elsewhere, details on the data-analysis are given in the results and discussion section.

D. Other Measurements

The thermal stability of the DDMS and OTS films is studied in an oxidizing ambient. This study is performed on single crystal Si(100) treated in a manner consistent with that described in the micromachine coating procedure. The heating setup for this series of experiments consists of a hotplate with a thick piece of machined aluminum fitted with a thermocouple at the surface. The aluminum slab is allowed to equilibrate to the desired temperature and the sample is placed upon the aluminum surface. The sample is exposed to high temperature, in laboratory air, for five minutes, and then removed to a room temperature aluminum slab for cooling. The five-minute exposure time is chosen based upon estimates of integrated circuit packaging times. The film stability is checked by contact angle goniometry, and the water contact angles are taken immediately after the samples cool.

Contact angle data are taken with DI water (resistivity 18 $\text{M}\Omega\text{-cm}$) and spectroscopic grade hexadecane (Aldrich Chemical Company) according to the sessile droplet method with a Ramé Hart 100 A goniometer. Droplet size is approximately $4\ \mu\text{l}$, and the measurement reproducibility is $\pm 2^\circ$. A digital instruments nanoscope III atomic force microscope is used in tapping mode to image the microstructure surfaces and quantify their roughnesses. All micromachine actuation is done under

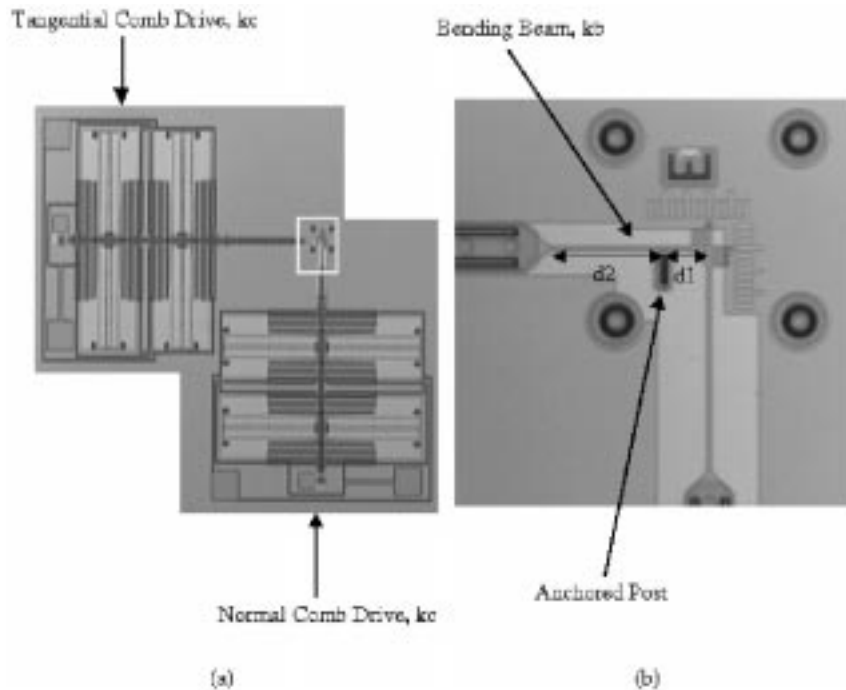


Fig. 3. Overall view of : (a) of the sidewall friction tester and close-up view (b) of the boxed area in (a), showing detail of the testing structure.

normal laboratory ambient conditions, 20 °C and 50% relative humidity. The probing system used for all micromachine actuation is a Lucas-Signatone S-1160 with a Mitutoyo FineScope 60 microscope, equipped with a Sony CCD-IRIS camera. A Nomarski style differential interference contrast prism (manufactured by Olympus) is used with a Mitutoyo M Plan Apo 10 \times objective on the microscope.

III. RESULTS AND DISCUSSION

A. Fill/Drain Approach to Solvent Reduction

In order to address the issue of large volumes of waste solvent generated by the displacement rinses commonly found in monolayer preparation procedures [8], [9], a solvent “fill/drain” approach is developed instead of an aspiration approach [17]. A schematic of an apparatus designed to accomplish this is shown in Fig. 1. Basically, this device consists of a Teflon FEP separatory funnel modified by cutting the top such that the rounded portion is removed. Also, a Teflon PFA plug is machined to fit inside the modified funnel so as to leave sufficient volume above the cone for process liquids. The plug reduces the amount of solvents needed, by reducing the stagnant volume of the funnel. Slots are cut into the Teflon plug to facilitate transfer of sample dies.

Since all the parts of the apparatus are made of some form of Teflon, any solvent or reagent of interest can be used with the funnel system. Since solvent displacements can occur within the same vessel, the need for sample transfers while maintaining a meniscus is greatly reduced. In order to displace one liquid with the next, the contents of the funnel are drained out (via the valve) until the liquid level is slightly above the sample die. Then the new solvent is poured into the top opening, mixed, and the funnel contents are drained out again. This process is repeated until the old solvent is completely displaced. When prop-

TABLE I
CONTACT ANGLE INFORMATION. THE MEASUREMENT
REPRODUCIBILITY IS ABOUT $\pm 2^\circ$

Surface Coating	Water Contact Angle	Hexadecane Contact Angle
DDMS	103°	38°
OTS	109°	38°
Oxide	0 – 30°	0 – 20°

erly performed, a single fill/drain cycle results in approximately one order of magnitude dilution of the old solvent with the new solvent. For example, to completely displace the concentrated HF etch solution (pH \sim 0) with deionized water (pH \sim 7) takes seven cycles, at about 50-mL water per cycle for a total of 350 mL for the displacement. Process run data indicate that the use of an apparatus like the one shown in Fig. 1 can reduce the total volume of chemical waste from some 6 l (generated by the aspiration process, described in [9]) to about 1.8 l. It should also be noted that much of this total volume is aqueous waste, and can be disposed of much more easily than organic waste. Additionally, due to the reduced handling of the sample dies, and the improved ability to displace solvents, the “fill/drain” approach may simplify the scale-up of anti-stiction monolayer processes to the wafer level.

B. Film Characteristics

Contact angle data for the DDMS coating are summarized in Table I. Also listed are the representative values for oxide and OTS coated surfaces for reference. The water contact angle data show that the DDMS film is not as hydrophobic as the OTS SAM. This result is expected, since, for DDMS, the methyl moieties present at the surface are not sufficiently distanced from

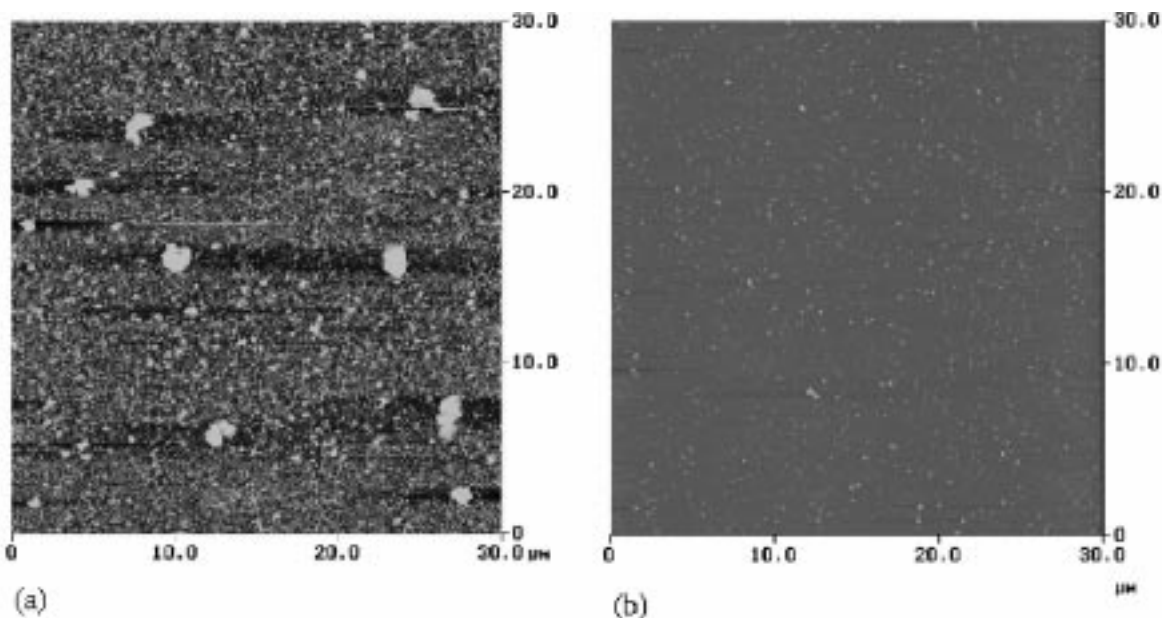


Fig. 4. AFM images of (a) an OTS SAM coated and (b) a DDMS coated Si(100) chip. The samples have undergone identical treatment as micromachine containing chips. The particulates on the surface are attributed to bulk polymerization of the precursor molecules. The rms roughness based on image statistics is 25 nm for (a) and 1.9 nm for (b). The z scale for both images is 100 nm.

the oxidized substrate to completely shield its hydrophilic effect. For OTS, the long chain (seventeen methylene groups) promotes self-assembly of the precursor molecules into a well packed monolayer that is methyl terminated. Hence, in the case of OTS, the methyl groups are far removed from the substrate, with the alkene chain providing effective screening of the hydrophilic properties of the oxide substrate. On the other hand, the hexadecane contact angles are the same for both OTS and DDMS films. Here, it must be kept in mind that the hexadecane experiences only van der Waals interactions with the surface. Therefore, contact angle analysis with hexadecane essentially probes the surface species. Since the hexadecane contact angles are about the same for both the OTS SAM and the DDMS monolayer, both surfaces most likely have similar densities of methyl groups.

AFM is used to study particulates that accumulate on the surface during the coating procedure. Fig. 4(a) and (b) shows AFM images for OTS and DDMS on Si(100) respectively. These samples have been treated alongside microstructures, and hence undergone every processing step exactly as the structures. The samples are not cleaned in any way after final removal from water. The scan size for both images is $30 \times 30 \mu\text{m}$. The z-range is 830 nm for the OTS scan and only 71 nm for the DDMS scan. Note that the OTS sample is cluttered with large particulates that are up to several microns in diameter. The rms roughness based on image statistics is 25 nm for the OTS sample and 1.9 nm for the DDMS sample. The particulates present on the surface are attributed to polymerization of the precursor molecules. The DDMS monolayer appears to have fewer and smaller particles, and this can be rationalized by considering that, after complete hydrolysis, the DDMS has only two silanol groups present whereas the OTS has three. Hence, the likelihood of polymerization for DDMS is much lower than for OTS.

It should be noted that there are means of reducing the particulate contamination seen with chlorosilane-based monolayers, by careful control of the coating process, and by meticulous handling of reagents and solvents that are used. The silane can be purified by distillation (atmospheric or vacuum depending on volatility), immediately before use to ensure that only monomer is present at the time of coating, and the entire procedure can be carried out in a dry-box with carefully controlled humidity. It must be kept in mind that some amount of water is required, because the first reaction step in the film formation process is the hydrolysis of the chlorosilane head group. However, too much water leads to bulk polymerization of the hydrolyzed precursor molecules. Thus, careful control of the amount of water present in the coating solution is critical. Additionally, high purity, anhydrous solvents can be used for rinses and the monolayer coating solution. However, these solvents are costly, and further purification steps are time consuming and must be carefully done. The anhydrous solvents must also be stored in a drybox, since they are hygroscopic. Special handling, expense, and other environmental constraints add to the difficulty of integrating the chlorosilane-based monolayers with industrial processes. All release processing for this study is carried out in a standard fume hood, with reagents used directly from the manufacturer. Thus, the reduction of particulate contamination witnessed by the DDMS coating is a significant advantage compared to the OTS SAM.

C. Micromachine Test Results

CBAs are used to find apparent work of adhesion values for the film. The work of adhesion can be found from this testing device in the following manner. Upon actuating all the beams, only those beams that are shorter than a characteristic length will have sufficient stiffness to free themselves completely from

TABLE II

DETACHMENT LENGTHS AND WORK OF ADHESION VALUES FOR DIFFERENT SURFACE COATINGS. UPON ACTUATION OF OXIDE COATED SAMPLES, ALL BEAMS REMAINED ADHERED TO THE SUBSTRATE. OXIDE VALUES GIVEN IN PARENTHESES ARE FROM [8], SINCE THE CANTILEVER BEAM ARRAYS USED IN THIS STUDY DID NOT PERMIT MEASUREMENT OF DETACHMENT LENGTH LESS THAN 150 μm

Surface Coating	Detachment Length (μm)	Work of Adhesion (\mathcal{W}) (mJ/m^2)	Standard Deviation on \mathcal{W}	μs	Standard Deviation on μs
DDMS	540	0.045	0.011	0.28	0.06
OTS	750	0.012	0.004	0.073	0.005
Oxide	< 150 (110)	>8 (20)		1.1	0.1

the substrate after the actuation force is removed. Beams longer than this characteristic length, however, will remain adhered to the surface. The value of this characteristic length, termed the detachment length ℓ_d is measured as the beam length at which the beams exhibit a transition from adhered to free standing. Based on this definition, the beams at the transition region are adhered to the substrate only at their tips, and by balancing the elastic energy stored within the beam and the beam-substrate interfacial energy, the work of adhesion \mathcal{W} between the two surfaces can be calculated using the following equation:

$$\mathcal{W} = \frac{3}{8} \frac{Eh^2t^3}{\ell_d^4} \quad (1)$$

where,

- E Young's modulus (~ 170 GPa for polysilicon [18]);
- h spacing between the beam and the substrate;
- t thickness of the polysilicon beams [13].

Details on the use of (1) and the numerical determination of the detachment length can be found elsewhere [9]. It should be noted that the detachment length is affected by on a multitude of factors, including roughness of contacting surfaces, the presence of strain gradients on the structural film and relative humidity. For these reasons, the detachment length, and therefore apparent work of adhesion, is not an absolute metric of performance for anti-stiction coatings. It is very useful, however, when comparing data collected on samples that are from the same fabrication run. Hence, care is taken to ensure that all the samples used in this study are from the same wafer.

After actuation, the beams are inspected to determine which ones are adhered to the substrate. Fig. 2 shows a picture of a typical post-release CBA as seen under differential contrast microscopy. Note that one beam appears substantially darker than the rest due to its adherence to the substrate. All the other beams in the picture are free standing. Due to the inherent variation from chip to chip, sticking probability data are accumulated over approximately 15 samples prepared independently by two operators. Detachment lengths, apparent work of adhesion, and standard deviation on the work of adhesion are summarized in Table II. Note that the detachment length associated with the DDMS coating is substantially lower than that for OTS, and that the resulting work of adhesion value for the DDMS coating is, on average, about four times greater than that of the OTS SAM. However, the DDMS still affords a vast improvement over the conventional oxidized surface, with a detachment

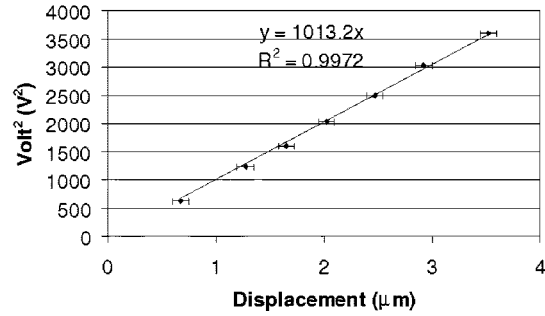


Fig. 5. Plot of V_{out}^2 versus axial displacement for the normal comb drive while bending the sidewall beam. The slope of this line is the ratio $(k_c + k_b)/a$. The value of δ_0 is $3.5 \mu\text{m}$. The linear fit equation and R^2 value for the fit is displayed on the plot. Voltages are measured with two decimal place accuracy. Displacement is measured optically with a resolution of ± 1 pixel, indicated by the error bars on displacement.

length of roughly five times greater than that of the oxide, which translates to a work of adhesion that is roughly three orders of magnitude less.

Sidewall friction testers are used to determine the coefficient of static friction on micromachine sidewalls, according to the following analysis. The force output of a set of interdigitated (comb) fingers is given by

$$F_{\text{out}} = \epsilon \frac{nh}{g} V^2 = aV^2$$

where

- n number of comb fingers;
- h thickness of the comb fingers;
- g actuation gap between the fingers;
- ϵ dielectric constant of the material between the fingers (in this case air);
- V applied voltage [19].

For simplicity, the constants are lumped into the parameter a . Since the displacement that results from actuation of a set of comb fingers within a comb drive results in an opposing force due to the folded beam suspensions within the comb drive, the force actually delivered by the comb drive is $F_{\text{delivered}} = F_{\text{out}} - k_c\delta$, where δ is the amount of displacement that the axis of the comb drive has undergone, and k_c is the effective spring constant for the folded beam suspension internal to the drive. Furthermore, the normal comb drive experiences an opposing force due to the normal deflection of the bending sidewall beam.

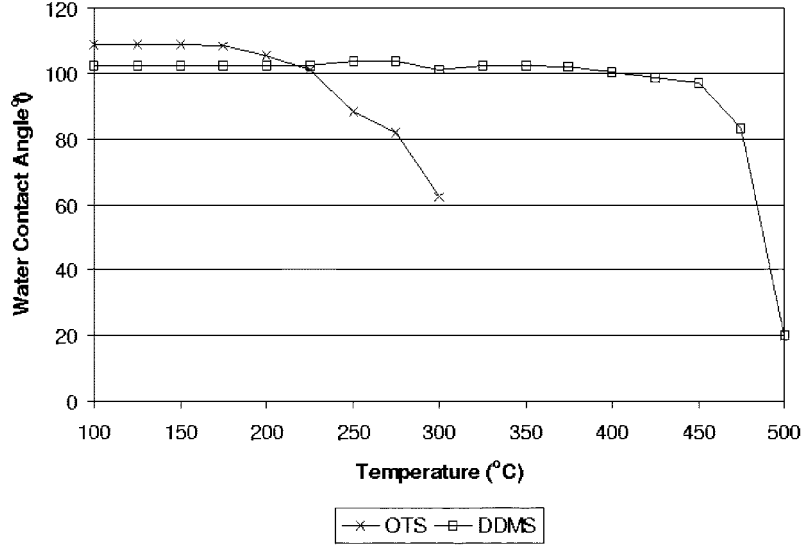


Fig. 6. Water contact angle as a function of exposure temperature in air. The substrate is Si(100), and the time of exposure is 5 minutes. Note that degradation of the OTS SAM begins to occur at about 225 °C, while the DDMS film does not begin to degrade until about 425 °C.

Hence, the force applied to the anchored post due to the normal comb drive can be expressed as

$$F_{\text{post}} = F_{\text{delivered}} - k_b \delta = a_N V_N^2 - \delta(k_c + k_b) \quad (2)$$

where k_b is an effective spring constant for the bending sidewall beam. The treatment of the folded beam suspensions and the sidewall beam bending as Hookean springs is only valid for small displacements. In the present device, the largest value that δ can acquire is the distance between the contacting surfaces of the sidewall beam and the anchored post when the device is in the unperturbed condition, namely δ_0 . This distance has been measured by optical microscopy on released devices at $3.5 \mu\text{m}$ (proof dimension is $3.0 \mu\text{m}$), which is rather small compared to the length of the folded beam suspension ($500 \mu\text{m}$) and the length of the bending sidewall beam ($86 \mu\text{m}$). When the device is in operation, the value of δ in (2) is δ_0 .

Since the device operates in a static mode, the summation of forces and the summation of moments must both be zero. This realization is important since the normal comb drive exerts not only a normal force onto the anchored post, but also creates a torque that must be balanced. The balancing torque must therefore be provided by the tangential comb drive, and results in a normally directed force on the anchored post with the magnitude $F_{\text{balance}} = (d_2/d_1)F_{\text{post}}$, where the dimensions d_2 and d_1 are given in Fig. 4. Hence, the total normal force exerted on the anchored post is

$$F_N = F_{\text{post}} + F_{\text{balance}} = \left(1 + \frac{d_2}{d_1}\right) [a_N V_N^2 - \delta_0(k_c + k_b)].$$

The tangential force is simpler to calculate, and is given by $F_T = a_T V_T^2$. Combining the formulations so far, the coefficient of static friction can be given as

$$\mu_S = \frac{F_T}{F_N} = \frac{a_T V_T^2}{\left(1 + \frac{d_2}{d_1}\right) [a_N V_N^2 - \delta_0(k_c + k_b)]} \quad (3)$$

In the case of identical normal and tangential comb drives, which is our case, $a_T = a_N = a$, and some rearrangement of (3) yields the following equation:

$$\mu_S = \frac{F_T}{F_N} = \frac{V_T^2}{\left(1 + \frac{d_2}{d_1}\right) \left(V_N^2 - \delta_0 \left(\frac{k_c + k_b}{a}\right)\right)} \quad (4)$$

Since d_1 , d_2 , and δ_0 can be measured optically with a microscope or found from the fabrication layout, the only unknown quantity in (4) is the ratio $(k_c + k_b)/a$. The value of this ratio can be determined by measuring the displacement as a function of applied potential on the normal comb drive as long as the sidewall beam does not touch the anchored post. Under these conditions, the force on the post is zero, and (2) becomes $V_N^2 = [(k_c + k_b)/a]\delta$. Hence, a plot of V_N^2 versus δ should yield a straight line with a slope of $(k_c + k_b)/a$ and an intercept of zero. It should be noted that this is a simple analysis, and that it is intended to serve only as a relative metric of μ_S .

In order to use (4), a value for the ratio $(k_c + k_b)/a$ is determined. Fig. 6 shows the plot of applied normal voltage squared (V_N^2) versus axial displacement of the normal comb drive (in microns) against the bending beam before the beam touches the anchored post. The linear fit to the data is forced to intercept the V_N^2 axis at zero. From this plot, the value of $1.01 \times 10^3 \text{ V}^2/\mu\text{m}$ is determined for $(k_c + k_b)/a$, and the coefficient of static friction calculations are performed in accordance with (4). Again, due to chip to chip variation, samples prepared by different operators are tested for each surface treatment. The results are summarized in Table II. Note that the DDMS treatment results in a surface that has a coefficient of static friction that is about four times that of the OTS SAM. However, both monolayers are highly favorable in comparison to the oxidized surface.

D. Thermal Stability

Perhaps the most compelling argument for use of the DDMS monolayer is its thermal stability. Fig. 6 shows a plot of water contact angle as a function of substrate temperature in air for

OTS- and DDMS-treated Si(100). Note that the DDMS treatment maintains a high ($> 100^\circ$) contact angle at temperatures of up to 400°C , and does not exhibit a sharp falloff in hydrophobicity until after 450°C . These results are consistent with earlier data reported for this system [12]. The OTS, however, begins to gradually degrade at about 200°C . These results can be rationalized as follows. Sung *et al.* have determined that the desorption mechanism for OTS in vacuum occurs by cleavage of the C-C bond within the alkyl chain, and continues until only a methyl group is present. This methyl group is strongly bound to the silicon oxide substrate, and remains on the surface up to about 620°C [20]. We suggest that the alkane chain of OTS becomes oxidized in a similar top down fashion upon heating in an oxidizing ambient. The DDMS, which has only methyl groups at the surface and no C-C bonds, is therefore immune to the effects of top down oxidation, and maintains its film characteristics over a wider temperature range.

IV. CONCLUSIONS

The DDMS monolayer is effective at alleviating the effects of release and in-use stiction, as evidenced by work of adhesion and friction measurements, compared to the oxide coating. The OTS SAM remains the better choice for solving the problems of stiction, owing to its lower apparent work of adhesion and coefficient of static friction. However, the OTS film may lose its effectiveness at reducing in-use stiction if it is exposed to temperatures in excess of 225°C in an oxidizing environment, whereas the DDMS film remains hydrophobic up to temperatures of 400°C . The DDMS molecule is less effective at polymerization. As a consequence, samples treated with the DDMS monolayer exhibit lower roughness due to fewer particulates than surfaces treated with the OTS SAM.

ACKNOWLEDGMENT

The authors wish to thank Dr. M. de Boer and Dr. J. Sniegowski of Sandia, for providing micromachine test structures and for many valuable discussions.

REFERENCES

- [1] Z. Rymuza, "Control tribological and mechanical properties of MEMS surfaces. Part I: Critical review," *Microsyst. Technol.*, vol. 5, pp. 173–180, 1999.
- [2] C. H. Mastrangelo, "Adhesion related failure mechanisms in micromechanical devices," *Tribology Lett.*, vol. 3, pp. 223–238, 1997.
- [3] R. Maboudian and R. T. Howe, "Critical review: Adhesion in surface micromechanical structures," *J. Vac. Sci. Technol. B*, vol. 15, pp. 1–20, 1997.
- [4] N. Tas, T. Sonnenberg, H. Jansen, R. Legtenberg, and M. Elwenspoek, "Stiction in surface micromachining," *J. Micromech. Microeng.*, vol. 6, pp. 385–397, 1996; and references therein.
- [5] K. Komvopoulos, "Surface engineering and microtribology for micromechanical systems," *Wear*, vol. 200, pp. 305–327, 1996.
- [6] B. Bhushan, *Tribology and Mechanics of Magnetic Storage Devices*. New York: Springer-Verlag, 1990.
- [7] R. L. Alley, G. J. Cuan, R. T. Howe, and K. Komvopoulos, "The effect of release-etch processing on surface microstructure stiction," in *Proc. IEEE Solid State Sensor and Actuator Workshop*, Hilton Head, SC, 1992, pp. 202–207.

- [8] M. R. Houston, R. T. Howe, and R. Maboudian, "Self-assembled monolayer films as durable anti-stiction coatings for polysilicon microstructures," in *Technical Digest of the 1996 Solid-State Sensor and Actuator Workshop*, Hilton Head, 1996, pp. 42–47.
- [9] U. Srinivasan, M. R. Houston, R. T. Howe, and R. Maboudian, "Alkyltrichlorosilane-based self assembled monolayer films for stiction reduction in silicon micromachines," *J. Microelectromech. Syst.*, vol. 7, June 1998.
- [10] J. B. Brzoska, L. Benazouz, and F. Rondelez, "Silanization of solid substrates—A step toward reproducibility," *Langmuir*, vol. 10, pp. 4367–4373, 1994.
- [11] W. R. Ashurst, C. Yau, C. Carraro, R. T. Howe, and R. Maboudian, "Alkene based monolayer films as anti-stiction coatings for polysilicon MEMS," in *Tech. Dig. 2000 Solid-State Sensor and Actuator Workshop*, pp. 320–323.
- [12] C. H. Oh, B. H. Kim, K. Chun, T. D. Chung, J. W. Byun, Y. S. Lee, and Y. S. Oh, "A new class of surface modification for stiction reduction," in *Technical Digest, Proceedings of the 10th International Conference on Solid-State Sensor and Actuators, Transducers '99*, pp. 30–33.
- [13] C. H. Mastrangelo, "A simple experimental technique for the measurement of the work of adhesion of microstructures," in *Proc. IEEE Solid State Sensor and Actuator Workshop*, Hilton Head, SC, 1992, pp. 208–212.
- [14] M. P. deBoer and T. A. Michalske, "Accurate method for determining adhesion of cantilever beams," *J. Appl. Phys.*, vol. 86, no. 2, pp. 817–827, 1999.
- [15] M. P. deBoer, P. J. Clews, B. K. Smith, and T. A. Michalske, "Adhesion of polysilicon microbeams in controlled humidity ambients," in *MRS Symp. Micromechanical Structures*, Spring 1998.
- [16] D. C. Senft and M. T. Dugger, "Friction and wear in surface micromachined tribological test devices," *SPIE*, vol. 3224, pp. 31–38, 1997.
- [17] R. Maboudian, W. R. Ashurst, and C. Carraro, "Self-assembled monolayers as anti-stiction coatings for MEMS: Characteristics and recent developments," *Sens. Actuators*, vol. 82, pp. 219–223, 2000.
- [18] B. D. Jensen, F. Bitsie, and M. de Boer, "Interferometric measurement for improved understanding of boundary effects in micromachined beams," *Micromachining and Microfabrication*, vol. 3875, pp. 61–72, 1999.
- [19] J. J. Sniegowski and E. J. Garcia, "Microfabricated actuators and their application to optics," in *Proc. SPIE Miniaturized Systems with Micro-Optics and Micromechanics*, San Jose, CA, 1995, pp. 46–64.
- [20] M. M. Sung, G. J. Kluth, O. W. Yauw, and R. Maboudian, "Thermal behavior of alkyl monolayers on silicon surfaces," *Langmuir*, vol. 13, no. 23, pp. 6164–6168, 1997.
- [21] R. Maboudian, "Surface processes in MEMS technology," *Surf. Sci. Reports*, 1998.

W. Robert Ashurst received the Bachelor's degree in chemical engineering from Auburn University, Auburn, AL, in 1998. He is currently working toward the Ph.D. degree in chemical engineering at the University of California, Berkeley. His research interests include the development and application of thin film coatings for microelectromechanical systems.

Christina Yau received the Bachelor's degree in bioengineering from the University of California, Berkeley, in 2000. She will join the joint bioengineering graduate program between University of California at Berkeley and San Francisco, to pursue the Ph.D. degree.

Carlo Carraro received the Bachelor's and Ph.D. degrees in chemical engineering, from the University of Padua, Padua, Italy, and the California Institute of Technology, Pasadena, respectively.

He is with the Department of Chemical Engineering at the University of California, Berkeley. His research interests include the physics of surfaces and surfactant thin films.

Roya Maboudian received the Ph.D. degree from the California Institute of Technology, Pasadena.

She is currently an Associate Professor in the Department of Chemical Engineering, University of California, Berkeley. Her research interests include the surface physics and chemistry of electronic materials. Her most recent work has focused on the problem of stiction in microelectromechanical systems. She and her group have designed surface processes to reduce adhesion and friction in MEMS. Maboudian is the recipient of several awards, including the Presidential Early Career Award for Scientists and Engineers, NSF Young Investigator award, the Beckman Young Investigator Award, the Alexander von Humboldt Fellowship, and IBM Postdoctoral Fellowship.

Michael T. Dugger received the B.S. and Ph.D. degrees, in metallurgical engineering and materials science, from the University of Illinois, Chicago, IL, and the Northwestern University, Chicago, IL, in 1984 and 1990, respectively.

He is currently a Principal Member of the Technical Staff at Sandia National Laboratories, performing research on solid lubricants, environmental effects in tribology, wear-resistant surface treatments, and molecular scale tribology of surface treatments for microsystems.